Selective Oxidation of Arabinose on Gold Catalysts

Hachhach, Mouad; Sladkovskiy, Dmitry A.; Salmi, Tapio; Murzin, Dmitry Y.

Published in:
Chemical Engineering and Technology

DOI:
10.1002/ceat.202100211

Published: 01/10/2021

Document Version
Final published version

Document License
CC BY

Mouad Hachhach[1]
Dmitry A. Sladkovskiy[2]
Tapio Salmi[1]
Dmitry Y. Murzin[1,*]

Selective Oxidation of Arabinose on Gold Catalysts: Process Design and Techno-economic Assessment

The present work focuses on process design and techno-economic assessment of the oxidation of a pentose sugar present in hemicelluloses, i.e., arabinose, on a supported gold catalyst. The processing plant was designed with Aspen Plus. The arabinose feedstock price has an important impact on the operational performance contributing to almost half of these costs. The feasibility of the overall arabinose oxidation process requires efficient extraction of hemicellulose from the lignocellulosic biomass lowering the feedstock costs.

Keywords: Arabinose oxidation, Gold catalysts, Process design, Techno-economic assessment

Received: May 18, 2021; *revised:* July 07, 2021; *accepted:* July 26, 2021

DOI: 10.1002/ceat.202100211

Supporting Information available online

1 Introduction

The strong dependence of the modern society on fossil feedstock for production of fuels, chemicals, and materials causes environmental, social, and political concerns for several reasons, including the global warming linked to emissions of greenhouse gases, such as CO_2 and NO_x [1]. On the contrary, biomass is a renewable raw material that can contribute to minimization of the global warming [2]. As an analogy to classical refineries, biorefineries are industrial facilities that convert almost all types of biomass into valuable products such as biofuels and chemicals [1]. One of the challenges in biomass processing is the feedstock chemical diversity.

Lignocellulosic biomass is of particular interest in the context of renewables, being able to meet requirements for both energy generation and synthesis of high value-added products. Moreover, this feedstock is non-edible, thus avoiding a controversial competition with agricultural commodities, which can be used for food purposes [3]. Lignocellulosic biomass comprises, besides cellulose, a polymer of glucose, also lignin, an alkylphenolic type of a polymer, and hemicelluloses. The latter is known as the second most abundant carbohydrate material and contributes to 25–35 % of the dry weight of wood [4].

Arabinose is an aldopentose obtained by hydrolysis of the hemicellulose arabinogalactan, which composes up to 15 % of softwoods and appears in large amounts in larch species (*Larix sibirica*) [5]. Extraction of arabinogalactan from larch wood chips and powder can be done in water at moderate temperatures at an industrial scale [5]. Arabinogalactan can be converted into valuable products through first its hydrolysis to monomers and subsequent transformations of the resulting sugars such as arabinose into bio-based products.

Selective oxidation of sugars over noble metal catalysis is one of the most important lignocellulosic biomass valorization processes along with hydrogenations and has been investigated extensively recently [6]. The oxidation reaction is accompanied by changes in pH generating a corresponding acid, influencing therefore activity and selectivity. An alternative option is to avoid the pH drift, in particular a constant addition of alkali such as sodium hydroxide keeps a constant pH favoring the cleavage of the ring and resulting in a salt (i.e., sodium arabinonate). More acidic conditions favor the formation of a lactone [7, 8].

Utilization of noble metals-based heterogeneous catalysis for selective oxidation of sugars in aqueous solutions has proved its potential, allowing high selectivity under mild conditions and diminishing formation of by-products, thus contributing to a more environmentally friendly process. Moreover, application of noble metal catalysis allows their reuse in batch reactors or stable operation in continuous reactors. In this context, utilization of gold is even more beneficial as it is not prone to over-oxidation, contrary to such noble metals as palladium or platinum [9].

Even if catalytic properties of gold were discovered a century ago [10, 11], it took many decades before a strong increase in the interest to this catalytic material and its application to a range of reactions took place [12, 13]. The critical aspects in

[1]Dr. Mouad Hachhach, Prof. Dr. Tapio Salmi, Prof. Dr. Dr. habil. Dmitry Y. Murzin
dmurzin@abo.fi
Åbo Akademi University, Johan Gadolin Process Chemistry Centre (PCC), Laboratory of Industrial Chemistry and Reaction Engineering, 20500 Turku/Åbo, Finland.

[2]Dr. Dmitry A. Sladkovskiy
St. Petersburg State Institute of Technology (Technical University), Moskovski pr. 26, 190013 Saint Petersburg, Russia.

catalysis by gold in terms of activity and selectivity are the size of gold clusters and the support, in particular the metal-support interactions. Gold on different oxides has been used for CO oxidation at low temperature since the late 1980s [14, 15]. The reaction scope was expanded to many oxidation reactions, including oxidative dehydrogenation of secondary alcohols, such as, e.g., a natural lignan hydroxymatairesinol [16] where gold on alumina was found to be the most efficient. More relevant in the context of this work is a study of Kusema et al. [17] who reported high catalytic activity and selectivity of gold nanoclusters supported on alumina in oxidation of arabinose under controlled basic pH and mild conditions in terms of pressure and temperature.

The aim of this work is to assess techno-economic feasibility of selective arabinose oxidation over gold on an alumina catalyst using available experimental data from the literature. Aspen Plus employed to design and simulate different chemical processes was chosen because of its ability to model complex processes using a simple graphical interface and a large database of compounds [18]. Moreover, this software is widely used in performing techno-economic assessment of various biomass conversion processes [19–23]. In the current work, Aspen Plus was applied for the design of a plant processing 3000 t a^{-1} of arabinose into arabinoic acid. The results served as a basis for the economic evaluation performed following the guidelines mentioned in the literature for similar cases [24–27].

2 Oxidation of Arabinose

Arabinose oxidation over gold catalysts was done isothermally at atmospheric pressure in a semi-batch mode [6] varying temperature, pH, and some catalytic properties to find the optimum reaction conditions. Kusema et al. [9] proved that in acidic media the maximum conversion of arabinose was only 23 % after 200 min giving just 46 % selectivity to the desired product with substantial amounts of the intermediate compound (arabinolactone) formed. On the contrary, in slightly basic media (pH 8–9) a complete conversion and total selectivity towards arabinoic acid was obtained after 200 min. As expected, the temperature elevation was beneficial for activity causing at the same time the formation of the undesired species [9].

The main product of the selective oxidation of arabinose over gold catalysts is the corresponding aldonic acid: arabinoic acid as shown in Fig. 1. The sugar acid and its derivatives found applications in the cosmetic, food, and pharmaceutical industries with competitive prices [28]. This figure illustrates the path for arabinose selective oxidation, through arabinolactone which is subsequently transformed into arabinoic acid [6].

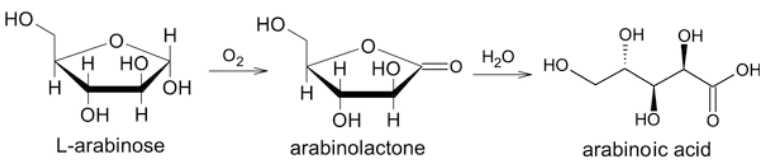

Figure 1. Reaction scheme for selective oxidation of arabinose over Au/Al_2O_3 (adapted from [29]).

While in the literature mainly batch reactors were reported for oxidation of sugars at laboratory scale, in the current study the continuous oxidation of arabinose over gold on an alumina catalyst was considered. Contrary to, e.g., continuous hydrogenation of sugars not requiring any pH adjustment, continuous oxidation can be more challenging because of the pH drift. An alternative approach would be to feed sodium hydroxide at several points along the reactor length. Van der Klis et al. [30] reported a possibility of continuous galacturonic acid oxidation using a plug-flow reactor without a pH control. Moreover, it was demonstrated that the selectivity in a plug-flow reactor was in the same range as in the batch reactor, namely, 94 and 99 mol %, respectively.

3 Process Scheme

The design was done for processing 3000 t a^{-1} of arabinose. Even if solubility of arabinose in water is rater high, i.e., 834 g L^{-1} at 25 °C, to avoid potential problems with solubility a safety margin should be added based on experience with hydrogenation of sugars. Thus, it was decided to use as a case study 30 % aqueous solution of arabinose implying feeding 3000 t a^{-1} of arabinose and 7000 t a^{-1} of water. This amount of feedstock was determined based on previous studies for similar products [31, 32].

A trickle-bed reactor with gold on an alumina catalyst was selected for arabinose oxidation, based on promising results in oxidation of sugars over such catalyst. Trickle-bed reactors are employed for hydrogenation of sugars such as arabinose [33] and in a range of industrial-scale oxidation reactions [34].

Kinetics and reaction conditions for oxidation of arabinose are typically studied in batch and semi-batch laboratory-scale reactors [6, 9], even if there are successful examples of continuous operation [30]. Bitter and co-workers [30] did not adjust the pH of the reaction media along the reactor length, thus operating in a pH drift mode. An alternative approach, as already mentioned, would be to adjust the pH by introducing an alkali solution, i.e., NaOH, at different points. In the current work aimed at techno-economic assessment of analysis, detailed reactor modeling was outside of the scope and only the option of adding sodium hydroxide at the inlet was considered.

Two scenarios of this study are defined for the production of arabinoic acid solution based on the heat recovery and reactor heating method, while the reaction conditions, temperature, pressure, feed stream composition, upstream process, and separation remained the same for both scenarios. The feedstock stream is composed of an aqueous solution of arabinose saturated with compressed air and solution of NaOH. The inlet temperature and pressure were 25 °C and 1 bar.

The first rather simple scenario is presenting the base case with neither heat recovery nor recycling. The feedstock passes through the adiabatic reactor before the phase separation using a flash separator. In the alternative case, the heat of the outlet stream of the adiabatic reactor is recuperated through a heat exchanger before the flash separation and is used to heat the inlet stream of the reactor. Flow sheets of the different scenarios are presented in Figs. 2 and 3.

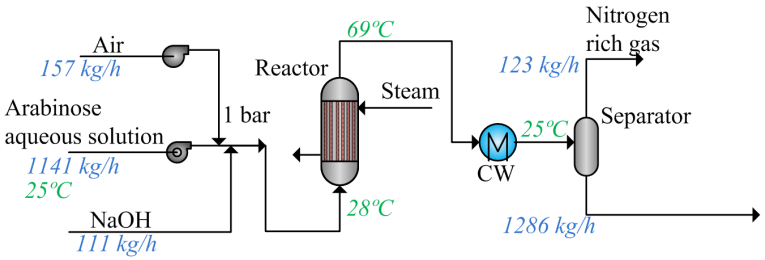

Figure 2. Flow sheet of arabinoic acid production (scenario 1).

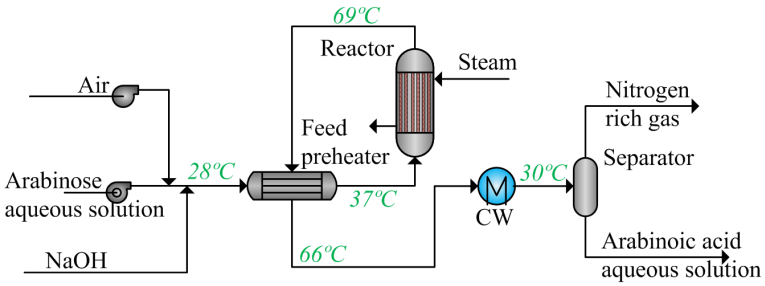

Figure 3. Flow sheet of arabinoic acid production (scenario 2).

3.1 Process Modeling and Simulation

Process modeling and simulation was done in the Aspen Plus V11 (Aspen Technology) environment previously used in similar cases [2, 20, 27, 35]. As arabinoic acid properties involved in modeling were not available in the Aspen Plus database, they were introduced to the simulation by a user-defined compound wizard option using a properties table as shown in Tab. 1 estimated via the Joback method [36]. Aspen Properties was employed to estimate the remaining parameters required for the simulations.

In this work, the Peng-Robinson equation of state (EoS) has been chosen to calculate the phase equilibrium for the whole system [37]. The Peng-Robinson method was developed first in 1976 making an additional improvement of the previous Redlich-Kwong cubic EoS to more accurately predict the vapor pressure, liquid density, and the equilibria ratios, for a large range of fluid mixtures including the nonpolar ones. The choice of such method is dictated by its applicability across a very broad temperature and pressure range not displaying any anomalous behavior, unlike the activity coefficient property method [38]. Moreover, this method has been used in the case studies [27, 35, 39] similar to the current work. The reactor was modeled using the Aspen PFR blocks, in line with Ranade et al. [34] who claimed that the plug-flow model is often applied for modeling of trickle-bed reactors. The kinetic data and stoichiometry of oxidation reactions were taken from [9].

Table 1. Reactant and product properties used for tuning the thermodynamic basis.

	Arabinose	Arabinoic acid
Molecular weight [g mol^{-1}]	150	166.13
Normal boiling point [°C]	441.86	554.1
Ideal liquid density [kg m^{-3}]	1571	1045
Critical temperature [°C]	617.3	739.7
Critical pressure [kPa]	6578	7548
Critical volume [m^{3}kg^{-1}mol^{-1}]	0.343	0.3985
Acentricity [–]	2.3	2.8

3.1.1 Upstream Feed

The inlet stream is composed mainly of the fresh reactants being identical for both scenarios. The sugar solution feed contains 30 wt % of arabinose with an annual flow rate of 10 kt. The sugar feed is then mixed first with the compressed flow of air (3 bar) to create a saturated solution, then with a strong base (NaOH) solution of 8.3×10^{-6} mol m^{-3} in a mixer operating at 25 °C and atmospheric pressure. The design specification block PHCNTRL was added to control the concentration of NaOH in order to keep a pH of 8 at the reactor output.

For the scenario 1, the feed stream goes directly to the reactor as explained previously, while for the scenario 2 there is a downstream unit which is composed of a plate and frame heat exchanger with an area of 1 m^2. The minimal temperature approach was taken as 10 °C and the overall heat transfer coefficient is 280 W m^{2}K^{-1}, where the heat from the reactor outlet stream is recovered to minimize the heat consumption and ensure a maximum temperature inside the reactor of 69 °C. In Aspen Plus the heat exchanger was simulated using the option HEATX with a minimum temperature specification of 10 °C. Design specification blocks were introduced in the Aspen Plus model to control the amount of the fresh feed avoiding accumulation of the unreacted reactants.

3.1.2 Reactor

A principal design of the reactor should be selected for the techno-economic assessment. The scaling-up of a reactor is always a challenging task which can be solved by building models based on experimental data similar to the methodology presented in [35].

The reactor unit is composed of a three-phase trickle-bed reactor with gold on alumina beads as a catalyst. Trickle-bed reactors are defined as continuous packed-bed reactors in which the liquid flows down through the packed catalyst bed in a trickling mode [40]. Such reactors are used in oxidation of sugars at the lab scale from the 1980s [41].

As mentioned above, selectivity and activity of gold-catalyzed oxidation are pH-dependent [42]. Interestingly enough, selectivity in the oxidation of galactogluronic acid on a gold catalyst even under pH drift is only slightly affected as 94 % selectivity was obtained in a continuous reactor with uncon-

trolled pH in comparison with 99 % for a batch reactor with controlled pH [30]. Kinetic models developed in the previous studies for gold catalysts [6, 9] can be used in a larger scale. The reactor modeling, however, should take into account internal and external mass transfer limitations, which is reflected by adjusting, e.g., the value of the activation energy compared to the batch reactor. It is worth mentioning that this adjustment of activation energy is not influencing the heat balance as the latter depends on the overall conversion [27].

The reactor unit was modeled as a plug-flow reactor (PFR) unit in Aspen Plus following some previous examples in modeling of catalytic trickle-bed reactors [43].

Similarly to experiments of Kusema et al. [9], complete conversion of sugars was reached in 100 min at 60 °C. The amount of reactants and catalyst used were scaled up linearly from the laboratory scale. It is noteworthy that to take into consideration the impact of mass transfer, the catalyst effectiveness factor was taken as 0.1. Thus, the overall catalyst load was 1041 kg with the volume of 1.63 m^3 considering the bulk density of 0.64 g cm^{-3} [6]. The reactor was considered as a vertical cylinder for both scenarios with the aspect ratio (length to diameter) equal to 3 [25] which results in a length of 3 m and a diameter of 1 m.

At the reactor outlet and for the residence time of 29 min, complete conversion of 3000 t a^{-1} of arabinose gives 11 263 t a^{-1} of arabinoic acid solution of 27 wt % (11 270 t a^{-1} for scenario 1). The rest is mainly composed of water and unreacted gaseous species as indicated in Tab. 2.

Table 2. Mass flow at the reactor outlet.

Compound	Mass flow [kg h^{-1}]
OH^-	1.55×10^{-5}
H_2O	909.194
Arabinoic acid	378.705
O_2	0
Na^+	2.095×10^{-5}
N_2	118.595
CO_2	0.079
Ar	2.016

3.1.3 Separation and Recycle

Separation of the arabinoic acid solution is done using the flash separation, allowing separation of arabinoic acid. The flash separators are known to operate at low temperature, opposite to some other unit operations used in similar cases, such as reactive distillation in lactic acid production [21], electrodialysis [44], and high-performance liquid chromatography for synthesis of lactobionic acid [45]. This can be translated into a decrease in the separation costs, which is essential since the separation and purification steps can contribute up to 50 % of the production costs [21, 46, 47].

To perform such separation in Aspen Plus, the "flash2" block was chosen. The flash separation is done under atmospheric pressure and with a flash temperature of 30 °C allowing separation of the excess of gaseous species and increasing the acid concentration in the final solution.

4 Process Cost Assessment

The economic assessment aims at giving an overview of the total costs (total capital investment and operating costs) of the selective oxidation of arabinose for a plant capacity of 11 270 t a^{-1} for the first scenario and 11 263 t a^{-1} for the second scenario. The calculated capital and operating costs are grouped in Tab. 3.

Table 3. Total capital and operating costs for different scenarios in M$.

	Scenario 1	Scenario 2
Total capital investment	1.26	1.28
Total operating costs	4.17	3.76

The cost estimation was done following the approach widely used in similar cases [25, 26] by dividing the costs into production and capital costs. The capital cost is calculated by summing the installed equipment costs taking into account a typical factor and reliable adjustments parameters. The estimation of the installed equipment costs was first carried out based on the previous Aspen Plus simulations results. The capital costs are divided into the fixed capital investment (FCI) and the working capital. FCI calculation is based on the purchase costs of the main equipment inside the battery limits (ISBL) while the other costs are estimated as a factor of the total equipment cost. The outside the battery limits (OSBL) are counted as 40 % of the FCI, construction and engineering costs amounting 30 % of the ISBL+OSBL, while contingency charges are 20 % of ISBL+OSBL. The working capital was estimated to be 15 % of ISBL+OSBL. Total capital investment TCI is the sum of FCI and the working capital.

The purchase equipment costs estimated based on the simulation results can be calculated using the correlations of the following simplified form [26]:

$$C_{PE} = (a + bS^n)f_m \quad (1)$$

where a and b are constants, S is the size parameter, n is the exponent, and f_m is the material cost factor being 1 for the carbon steel case and 1.3 for stainless steel used in the arabinoic acid production case. The values of constants depend on the equipment type and can be retrieved from Sinott et al. [26], where the purchase costs are referred to Gulf Coast basis as of January 2006 (CEPCI = 478.6).

The installed equipment costs C_{IE} were estimated from the following equation:

$$C_{IE} = C_{PE}f_i\frac{CEPCI(2019)}{CEPCI(old)} \quad (2)$$

where f_i is the Hand's installing factor (4 for vessels and reactor, 3.5 for heat exchanger, 2.5, 2 for heaters, and 2.5 for the remaining equipment) [26]. The costs were adjusted to 2019 (CEPCI 2019 = 607.5) [48].

The reactor total purchase cost is assumed to include the cost of shell and the catalyst bed. The recovery rate of gold in the catalyst was assumed to be 96 %, thus the only costs of the gold in the catalyst accounted are the non-recovered 4 % while the remaining metal can be completely recovered allowing complete cost compensation at the end of the catalyst lifetime. The costs of gold recovery are divided into the reclamation costs taken 3.3 $ kg^{-1} and the preprocessing costs equal to 1.3 $ kg^{-1} according to Dutta et al. [49]. Based on that, the capital cost of the reactor is estimated to be ca 68 k$. Taken into account that the price of the support and the catalyst preparation was considered to be 50 $ kg^{-1}, the total catalyst cost was then estimated to be 54 057 $ using the gold price of 1850 $ kg^{-1}. The required catalysts amounts have been calculated based on the available experimental data. It is worth mentioning that the values might be somewhat underestimated which can slightly increase the catalyst load and the reactor volume [27].

Similar to the reactor, the flash separator cost is assumed to include the shell (vertical pressure vessel). The costs of this and other pieces of equipment are given in the Supporting Information.

The production costs (TCOP) are composed of the variable costs of production (VCOP), also known as the operating costs, fixed costs of production (FCOP), and the annual capital charge (ACC) [26]:

$$\mathrm{TCOP} = \mathrm{VCOP} + \mathrm{FCOP} + \mathrm{ACC} \quad (3)$$

$$\mathrm{ACC} = \mathrm{FCI} \times \mathrm{ACCR} \quad (4)$$

where ACCR is the annual capital charge ratio. In this work, ACCR was taken as 0.16 corresponding to the interest rate of 15 % [26, 35] and the plant life time as 20 years.

The variable production cost calculations were done with the following cost factors: 7.78 $ GJ^{-1} for the low-pressure steam, 0.056 $ kWh^{-1} for electricity, 1.776 $ t^{-1} for water, and 3 $ t^{-1} for the wastewater treatment. The feedstock arabinose price was set at 625 $ t^{-1} (dry basis) [27]. Oxygen costs were taken as 87 $ t^{-1} [50] while the costs of NaOH were 14 $ kg^{-1}. The fixed costs include the operating labor (three shift positions in three shifts, with an average yearly wage per person of 75 000 $). The remaining operating cost components (i.e., maintenance, overheads, taxes, and insurance, general expenses) were estimated based on percentages from the known parameters using the factors from Peters et al. [24] as specified in Tab. 4 and mentioned in the previous work [20]. Moreover, 10 years straight-line depreciation was considered, and the rent of land was assumed equal to 2 % of ISBL+OSBL.

The total annual operating costs are summarized in Tabs. S2 and S5 in the Supporting Information. The cost of the acid was either 370 or 314 $ t^{-1} of an arabinoic acid solution of 29 wt % for scenarios 1 and 2, respectively. It is heavily dependent on the arabinose feedstock exhibiting alone above 46 % of the TCOP, highlighting clearly a need to diminish the production costs of the upstream processes, namely, extraction of hemicelluloses from lignocellulosic biomass and its subsequent hydrolysis.

Table 4. Summary of calculation factors for operating costs.

Operating costs	Definition
Variable costs	
Raw materials (RM)	Calculated
Utilities (U)	Calculated
Fixed costs	
Operating labor (OL)	Calculated
Operating supervision (S)	15 % of OL
Laboratory charges	15 % of OL
Maintenance (M)	4 % of FCI
Operating supplies	15 % of M
Plant overheads	60 % of (OL+S+M)
Taxes and insurance	3 % of FCI
Land	2 % ISBL+OSBL
General expenses	5 % of variable + fixed
Annual capital charge	
Total operating cost	Variable + fixed + general expenses + annual charges

The profitability of the process is assessed through calculation of the key indicators such as NPV (net present value), ROI (return on investment), and PBP (payback period). Moreover, the following assumptions were used to perform discounted cash flow analysis: the plant is assumed to be located in Finland, and thus, the corporate tax is taken ca 20 %. The discount rate was set to 15 % and the interest rate is 10 % for a 20-year plant life [51]. Construction and starting of the plant will take two years, thus, TCI will be spent in that period, while at the end of the plant life time the working capital (WC) will be recovered. The plant will achieve 100 % of production capacity during its first year after construction.

For straight-line depreciation calculation, the equipment lifetime is 10 years; the salvage value was taken as zero, e.g., the fixed capital investment of the plant minus the value of the land, evaluated at the end of the plant life. The land costs constitute 2 % of the FCI. The revenues of this process are assumed to originate only from selling arabinoic acid solution at the market price taken as 0.4 $ kg^{-1}. The latter value is lower than the price of a commercially available solution of arabinoic acid [52] as when a technology for producing of the acid is evolving, the costs are anticipated to decrease. The equations used to perform the calculations are grouped in the Supporting Information.

The calculation of the profitability indexes (NPV, ROI, and PBP) is summarized in Tab. 5, while the cash flow tables for both scenarios can be found in the Supporting Information (Tabs. S3 and S6). Tab. 5 and Fig. 4 show that scenario 2 is the most profitable illustrating that profitability is strongly influ-

Table 5. Profitability indexes calculations.

	Scenario 1	Scenario 2
NPV [$]	1 103 530	3 905 460
ROI [%]	16.2	57.9
PBP [years]	6.2	1.8

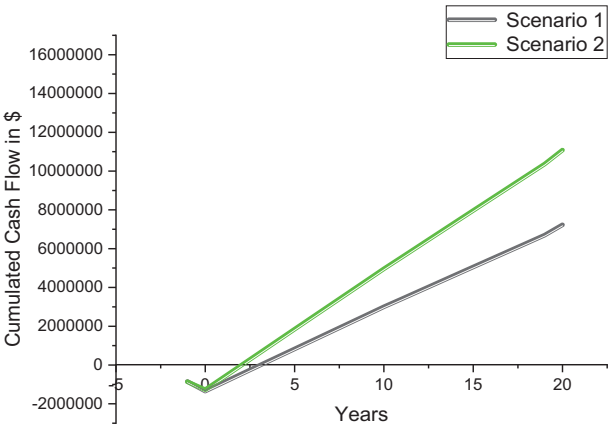

Figure 4. Cumulated cashflow for different scenarios.

enced by the operating costs, which are highly dependent on the arabinose feedstock.

5 Conclusions

The present study reports the techno-economic assessment of arabinose oxidation to arabinoic acid including the cost estimation for the industrial process and a profitability assessment. The process design was based on the experimental data for arabinose oxidation at ca 70 °C and atmospheric pressure over a 2 % Au/Al_2O_3 catalyst. The process model was built using Aspen Plus to process 3000 t a^{-1} of neat arabinose. Two scenarios were adopted depending on the heat recovery method, i.e., the base scenario without any heat recovery and the second one with heat recuperation through a heat exchanger. The total production costs were calculated as high as 4.2 M$ a^{-1} with the capital costs up to ca 1.7 M$.

The production costs strongly influence the profitability of the process being mainly related to the feedstock price, therefore, arabinose should be produced from a relatively cheap renewable source. This indicates the importance of developing an economic process for extraction of hemicelluloses containing arabinose, e.g., arabinogalactan, from lignocellulosic biomass.

Supporting Information

Supporting Information for this article can be found under DOI: https://doi.org/10.1002/ceat.202100211.

Acknowledgment

This work is part of the activities of the Åbo Akademi Process Chemistry Center (PCC), a center of excellence for scientific research. The financial support obtained from PCC, Otto A. Malm Foundation, Walter Ähllstrom Foundation, and from The Society of Swedish Literature in Finland (SLS) to M. Hachhach is gratefully acknowledged.

The authors have declared no conflict of interest.

Symbols used

a	[–]	constant
ACC	[–]	annual capital charge
ACCR	[–]	annual capital charge ratio
b	[–]	constant
C_{IE}	[$]	installed equipment cost
C_{PE}	[$]	purchased equipment cost
CEPCI	[–]	chemical engineering plant cost index
f_i	[–]	Hand's installing factor
f_m	[–]	material cost factor
FCI	[$]	fixed capital investment
FCOP	[$]	fixed costs of production
n	[–]	exponent
NPV	$	net present value
PBP	[a]	payback period
ROI	[%]	return on investment
S	[–]	size parameter
TCI	[$]	total capital investment
TCOP	[$]	total costs of production
VCOP	[$]	variable costs of production
WC	[$]	working capital

Abbreviations

EoS	equation of state
ISBL	inside battery limits
NO_x	nitrogen oxides
OSBL	outside battery limits
PFR	plug-flow reactor

References

[1] F. Cherubini, *Energy Convers. Manage.* **2010**, *51 (7)*, 1412–1421. DOI: https://doi.org/10.1016/j.enconman.2010.01.015

[2] J. Moncada, I. Vural Gursel, W. J. J. Huijgen, J. W. Dijkstra, A. Ramírez, *J. Cleaner Prod.* **2018**, *170*, 610–624. DOI: https://doi.org/10.1016/j.jclepro.2017.09.195

[3] T. H. Mekonnen, M. Misra, A. K. Mohanty, in *Biocomposites: Design and Mechanical Performance* (Eds: M. Misra, J. Pandey, A. Mohanty), Elsevier, New York **2015**.

[4] N. Ahmad, M. R. Zakaria, in *Lignocellulose for Future Bioeconomy* (Eds: H. Ariffin, S. M. Sapuan, M. Ali Hassan), Elsevier, New York **2019**.

[5] P. Mäki-Arvela, T. Salmi, B. Holmbom, S. Willför, D. Y. Murzin, *Chem. Rev.* **2011**, *111 (9)*, 5638–5666. DOI: https://doi.org/10.1021/cr2000042

[6] L. S. Correia, H. Grénman, J. Wärnå, T. Salmi, D. Y. Murzin, *Chem. Eng. J.* **2019**, *370*, 952–961. DOI: https://doi.org/10.1016/j.cej.2019.03.241

[7] A. M. Cañete-Rodríguez, I. M. Santos-Dueñas, J. E. Jiménez-Hornero, A. Ehrenreich, W. Liebl, I. García-García, *Process Biochem.* **2016**, *51 (12)*, 1891–1903. DOI: https://doi.org/10.1016/j.procbio.2016.08.028

[8] N. Bhagavan, *Medical Biochemistry*, 4th ed., Academic Press, New York **2002**.

[9] B. T. Kusema, J. P. Mikkola, D. Y. Murzin, *Catal. Sci. Technol.* **2012**, *2 (2)*, 423–431. DOI: https://doi.org/10.1039/c1cy00365h

[10] E. Behravesh, N. Kumar, Q. Balme, J. Roine, J. Salonen, A. Schukarev, J. P. Mikkola, M. Peurla, A. Aho, K. Eränen, D. Murzin, T. Salmi, *J. Catal.* **2017**, *353*, 223–238. DOI: https://doi.org/10.1016/j.jcat.2017.07.014

[11] S. J. Fokin, *Russ. J. Phys. Chem.* **1913**, *45*, 286–288.

[12] D. T. Thompson, *Nano Today* **2007**, *2 (4)*, 40–43. DOI: https://doi.org/10.1016/S1748-0132(07)70116-0

[13] G. C. Bond, D. T. Thompson, *Gold Bull.* **2000**, *33 (2)*, 41–50. DOI: https://doi.org/10.1007/BF03216579

[14] M. Haruta, N. Yamada, T. Kobayashi, S. Iijima, *J. Catal.* **1989**, *115 (2)*, 301–309. DOI: https://doi.org/10.1016/0021-9517(89)90034-1

[15] M. Haruta, T. Kobayashi, H. Sano, N. Yamada, *Chem. Lett.* **1987**, *16 (2)*, 405–408. DOI: https://doi.org/10.1246/cl.1987.405

[16] O. A. Simakova, E. V. Murzina, P. Mäki-Arvela, A. R. Leino, B. C. Campo, K. Kordás, S. M. Willför, T. Salmi, D. Y. Murzin, *J. Catal.* **2011**, *282 (1)*, 54–64. DOI: https://doi.org/10.1016/j.jcat.2011.05.025

[17] B. T. Kusema, B. C. Campo, P. Mäki-Arvela, T. Salmi, D. Y. Murzin, *Appl. Catal., A* **2010**, *386 (1–2)*, 101–108. DOI: https://doi.org/10.1016/j.apcata.2010.07.037

[18] M. Hachhach, H. Akram, M. Hanafi, O. Achak, T. Chafik, *Int. J. Chem. Eng.* **2019**, 3953862. DOI: https://doi.org/10.1155/2019/3953862

[19] K. K. Kapanji, K. F. Haigh, J. F. Görgens, *Bioresour. Technol.* **2019**, *289*, 121635. DOI: https://doi.org/10.1016/j.biortech.2019.121635

[20] I. Vural Gursel, J. W. Dijkstra, W. J. J. Huijgen, A. Ramirez, *Biofuels, Bioprod. Biorefin.* **2019**, *13 (4)*, 1068–1084. DOI: https://doi.org/10.1002/bbb.1999

[21] A. Gezae Daful, J. F. Görgens, *Chem. Eng. Sci.* **2017**, *162*, 53–65. DOI: https://doi.org/10.1016/J.CES.2016.12.054

[22] G. Bagnato, A. Sanna, *Catalysts* **2019**, *9 (12)*, 1021. DOI: https://doi.org/10.3390/catal9121021

[23] D. J. Lundberg, D. J. Lundberg, M. A. Hillmyer, P. J. Dauenhauer, *ACS Sustainable Chem. Eng.* **2018**, *6 (11)*, 15316–15324. DOI: https://doi.org/10.1021/acssuschemeng.8b03774

[24] *Plant Design and Economics for Chemical Engineers* (Eds: M. S. Peters, K. D. Timmerhaus, R. E. West), 5th ed., Vol. 66, McGraw-Hill, New York **2003**.

[25] *Analysis, Synthesis, and Design of Chemical Processes* (Eds: R. Turton, J. A. Shaeiwitz, D. Bhattacharyya, W. B. Whiting), 5th ed., Prentice Hall, Boston, MA **2018**.

[26] *Chemical Engineering Design: Principles, Practice and Economics of Plant and Process Design* (Eds: G. Towler, R. Sinnott), 2nd ed., Butterworth-Heinemann, Oxford **2013**.

[27] D. Y. Murzin, E. Daigue, R. Slotte, D. A. Sladkovskiy, T. Salmi, *Chem. Eng. Technol.* **2020**, *43 (7)*, 1260–1267. DOI: https://doi.org/10.1002/ceat.202000125

[28] F. W. Lichtenthaler, Carbohydrates as Organic Raw Materials, in *Ullmann's Encyclopedia of Industrial Chemistry*, Wiley-VCH, Weinheim **2010**. DOI: https://doi.org/10.1002/14356007.n05_n07

[29] S. Franz, N. D. Shcherban, I. Bezverkhyy, S. A. Sergiienko, I. L. Simakova, T. Salmi, D. Y. Murzin, *Res. Chem. Intermed.* **2021**, *47 (6)*, 2573–2587. DOI: https://doi.org/10.1007/s11164-021-04426-6

[30] F. Van Der Klis, L. Gootjes, J. Van Haveren, D. S. Van Es, J. H. Bitter, *React. Chem. Eng.* **2018**, *3 (4)*, 540–549. DOI: https://doi.org/10.1039/c8re00047f

[31] Ç. Efe, L. A. M. van der Wielen, A. J. J. Straathof, *Biomass Bioenergy* **2013**, *56*, 479–492. DOI: https://doi.org/10.1016/j.biombioe.2013.06.002

[32] I. Bechthold, K. Bretz, S. Kabasci, R. Kopitzky, A. Springer, *Chem. Eng. Technol.* **2008**, *31 (5)*, 647–654. DOI: https://doi.org/10.1002/ceat.200800063

[33] V. Russo, T. Kilpiö, M. Di Serio, R. Tesser, E. Santacesaria, D. Y. Murzin, T. Salmi, *Chem. Eng. Res. Des.* **2015**, *102*, 171–185. DOI: https://doi.org/10.1016/j.cherd.2015.06.011

[34] *Trickle Bed Reactors* (Eds: V. Ranade, R. Chaudhari, P. R. Gunjal), Elsevier, New York **2011**.

[35] D. A. Sladkovskiy, L. I. Godina, K. V. Semikin, E. V. Sladkovskaya, D. A. Smirnova, D. Y. Murzin, *Chem. Eng. Res. Des.* **2018**, *134*, 104–116. DOI: https://doi.org/10.1016/j.cherd.2018.03.041

[36] K. G. Joback, R. C. Reid, *Chem. Eng. Commun.* **1987**, *57 (1–6)*, 233–243. DOI: https://doi.org/10.1080/00986448708960487

[37] D. Y. Peng, D. B. Robinson, *Ind. Eng. Chem. Fundam.* **1976**, *15 (1)*, 59–64. DOI: https://doi.org/10.1021/i160057a011

[38] Aspen Physical Property System, Physical Property Methods and Models 11.1, Aspen Technology Inc., Bedford, MA **2001**.

[39] A. Athaley, P. Annam, B. Saha, M. Ierapetritou, *Comput. Chem. Eng.* **2019**, *121*, 685–695. DOI: https://doi.org/10.1016/j.compchemeng.2018.11.018

[40] P. C. Munasinghe, S. K. Khanal, *Bioresour. Technol.* **2010**, *101 (13)*, 5013–5022. DOI: https://doi.org/10.1016/j.biortech.2009.12.098

[41] T. Tsukamoto, S. Morita, J. Okada, *Chem. Pharm. Bull.* **1983**, *31 (11)*, 3785–3795. DOI: https://doi.org/10.1248/cpb.31.3785

[42] U. Prüße, S. Heidinger, C. Baatz, *Landbauforsch.* **2011**, *3 (61)*, 261–272.

[43] I. Bergault, M. V. Rajashekharam, R. V. Chaudhari, D. Schweich, H. Delmas, *Chem. Eng. Sci.* **1997**, *52*, 4033–4043.

[44] F. A. Peretti, M. M. Silveira, M. Zeni, *Desalination* **2009**, *245 (1–3)*, 626–630. DOI: https://doi.org/10.1016/j.desal.2009.02.029

[45] P. J. Simms, K. B. Hicks, R. M. Haines, A. T. Hotchkiss, S. F. Osman, *J. Chromatogr. A* **1994**, *667 (1–2)*, 67–73.

[46] C. Y. Su, C. C. Yu, I. L. Chien, J. D. Ward, *Ind. Eng. Chem. Res.* **2013**, *52 (32)*, 11070–11083. DOI: https://doi.org/10.1021/ie303192x
[47] K. L. Wasewar, *Chem. Biochem. Eng. Q.* **2005**, *19 (2)*, 159–172.
[48] www.chemengonline.com/2019-chemical-engineering-plant-cost-index-annual-average/ (Accessed on January 19, 2021)
[49] A. Dutta, J. A. Schaidle, D. Humbird, F. G. Baddour, A. Sahir, *Top. Catal.* **2016**, *59 (1)*, 2–18. DOI: https://doi.org/10.1007/s11244-015-0500-z
[50] M. Hurskainen, *Industrial Oxygen Demand in Finland*, VTT Research Report No. VTT-R-06563-17, VTT Technical Research Centre of Finland, Espoo **2017**.
[51] M. M. Wright, J. A. Satrio, R. C. Brown, D. E. Daugaard, D. D. Hsu, *Fuel* **2010**, *89 (S1)*, S2–S10.
[52] www.alibaba.com/product-detail/High-quality-99-D-Arabonic-acid_60822591094.html?spm=a2700.galleryofferlist.normal_offer.d_title.6dfd6342h0Uzda (Accessed on January 19, 2021)

